SUPPLEMENTARY INFORMATION

NLRP3, conveyed via extracellular vesicles from metabolic syndrome patients, is involved in atherosclerosis development

Xavier Vidal-Gómez[1,2]; Luisa Vergori[2]; Severine Dubois[3]; Frédéric Gagnadoux[2,3]; Samir Henni[3]; Reuben Veerapen[4]; Olivier Meilhac[5]; Mercedes Muñoz-Picos[2]; Concepción Peiró[6]; M Carmen Martinez[1,2]; Ramaroson Andriantsitohaina*[1,2]; On behalf of Metabol Study Group

Contents:

Supplementary Table 1. Pearson correlation coefficients (r-value) for the relation of plasma circulating lEVs (Total lEVs) and sEVs (Total sEVs) with the clinical parameters of all the subjects used in the present study. r-values and p-values in bold are considered statistically significant (p-value ≤ 0.05). BMI = Body mass index, HbA1c = glycated haemoglobin, CRP = C-reactive protein

	Total lEVs			Total sEVs		
	n	r-value	p-value	n	r-value	p-value
Anthropomorphic parameters						
Age (years)	49	-0.1494	0.3056	44	-0.2700	0.0746
Body weight (kg)	49	0.0933	0.5238	44	0.1000	0.5093
Height (cm)	49	-0.0650	0.6571	44	-0.1100	0.4685
Waist circumference (cm)	49	0.0531	0.7169	44	0.1500	0.3421
Hip circumference (cm)	49	0.1071	0.4640	44	0.1300	0.4147
BMI (kg/m^2)	49	0.1151	0.4312	44	0.1900	0.2145
Cardiovascular parameters						
Systolic blood pressure (mmHg)	49	0.1874	0.1973	44	0.2300	0.1325
Diastolic blood pressure (mmHg)	**49**	**0.3369**	**0.0179**	44	0.2300	0.1390
Heart rate (bpm)	47	0.0326	0.8276	42	0.1700	0.2756
Metabolic parameters						
HbA1c (% of total Hb)	48	-0.0801	0.5885	43	0.0200	0.8891
Glycemia (g/L)	49	0.2102	0.1471	**44**	**0.3300**	**0.0292**
Insulinemia (mU/L)	**11**	**0.8793**	**0.0004**	11	0.3800	0.2541
HOMA index	**11**	**0.8700**	**0.0005**	11	0.3800	0.2471
CRP (mg/L)	8	-0.1407	0.7397	8	0.1100	0.8005
Lipid profile						
Total cholesterol (g/L)	49	0.0262	0.8583	44	0.0410	0.7937
HDL-cholesterol (g/L)	49	-0.1317	0.3669	44	-0.2400	0.1159
LDL-cholesterol (g/dL)	49	-0.0976	0.5048	44	0.0480	0.7554
Triglycerides (g/dL)	**49**	**0.3212**	**0.0244**	44	0.1800	0.2490
Cardiovascular risk						
Triglyceride/Glucose ratio	49	0.1502	0.3030	44	0.1900	0.2074
Triglyceride/HDL-c ratio	49	0.2773	0.0538	44	0.2000	0.2011

Supplementary Table 2. Non-significant Pearson correlation coefficients (r-value) for the relation of plasma circulating NLRP3^{+} lEVs with clinical parameters of all the subjects used in the present study. No correlations of circulating NLRP3+ sEVs were evaluated. r-values and p-values in bold are considered statistically significant (p-value ≤ 0.05).

	NLRP3^{+} lEVs		
	n	r-value	p-value
Anthropomorphic parameters			
Age (years)	49	-0.1685	0.2471
Height (cm)	49	-0.0912	0.5339
Cardiovascular parameters			
Systolic blood pressure (mmHg)	49	0.1514	0.2991
Heart rate (bpm)	47	0.1479	0.3213
Lipid profile			
Total cholesterol (g/L)	49	-0.0918	0.5306
LDL-cholesterol (g/dL)	49	-0.1678	0.2491

Supplemental Figure 1
(Vidal-Gomez et al.)

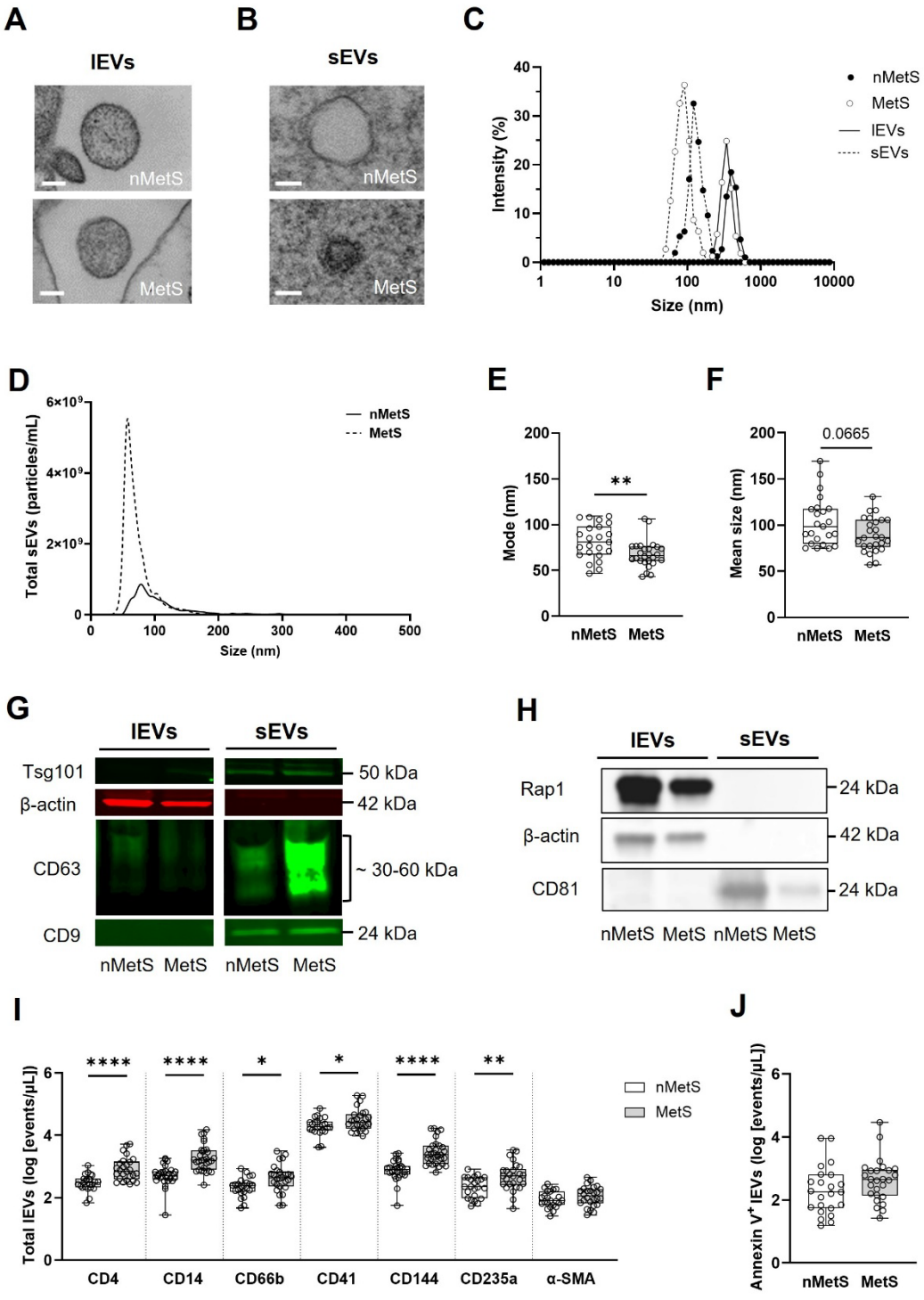

Supplementary Figure 1. Characterization of lEVs and sEVs from non-metabolic syndrome (nMetS) subjects and metabolic syndrome (MetS) patients. A-B, Representative transmission electron microscopy images of lEVs (A) and sEVs (B).

Scale-bar size: 200 and 50 nm, respectively. C, Representation of the mean size distribution of lEVs and sEVs from nMetS subjects (n=3) and MetS (n=3) patients analyzed by Zeta-sizer Nano. D, Graphical representation of the mean size distribution profile obtained by nanotracking analysis (NTA) of purified sEVs from a nMetS subject (0 criterion) and a MetS patient (5 criteria). E and F, NTA resulting values of mode (E) and mean (F) size of circulating sEVs from nMetS (n=23) and MetS (n=26) patients. G and H, Representative blot images of differential expression of specific EV markers on nMetS and MetS samples. I and J, Cellular origins (I) and annexin V^+ (pro-coagulant EVs, J) of lEVs from nMetS (n=23) and MetS (n=26) patients. Data are shown as medians and interquartiles of the log of [lEVs/µL]. Mann-Whitney U test for E and F, and unpaired Student's t-test for I to J. *p<0.05, **p<0.01, and ****p<0.0001.

Supplemental Figure 2
(Vidal-Gomez et al.)

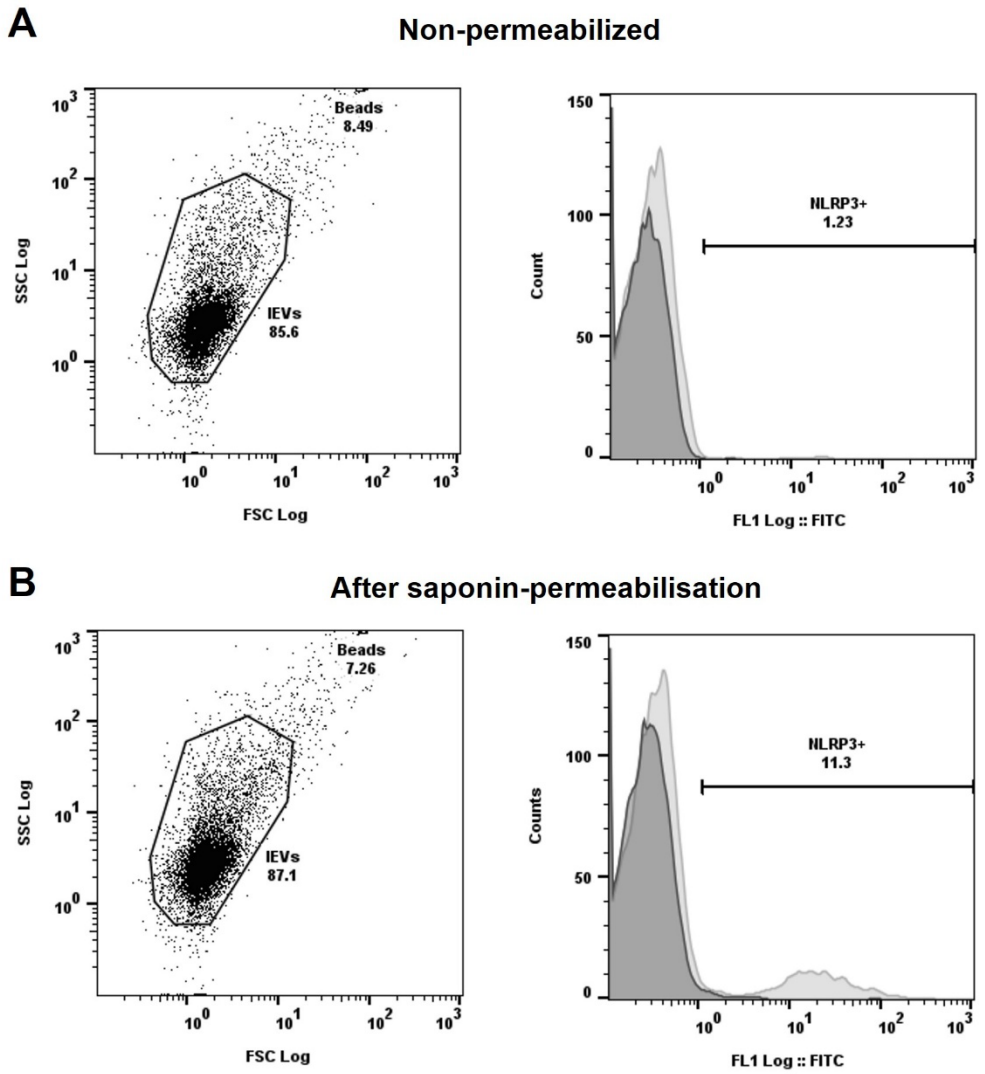

Supplementary Figure 2. Flow cytometry gating strategy for NLRP3^{+}-large EVs (lEVs) numeration and specific markers expression. Non-permeabilized (A) or permeabilized plasmatic lEVs after treatment with saponin (B) and counting beads (beads, 10 µm diameter) are visualized in a side scatter/forward scatter logarithmic representation (SSC Log vs. FSC Log) and the resulting NLRP3-labelling analysis. lEVs are defined as events with size 0.1 to 1 mm gated in the “lEVs” window. The percentages show the number of positive events for staining of plasma lEVs visualized

by plotting NLRP3 marker (light gray) (*x*-axis) versus total events (*y*-axis) and gated based on isotype control (dark gray).

Supplemental Figure 3
(Vidal-Gomez et al.)

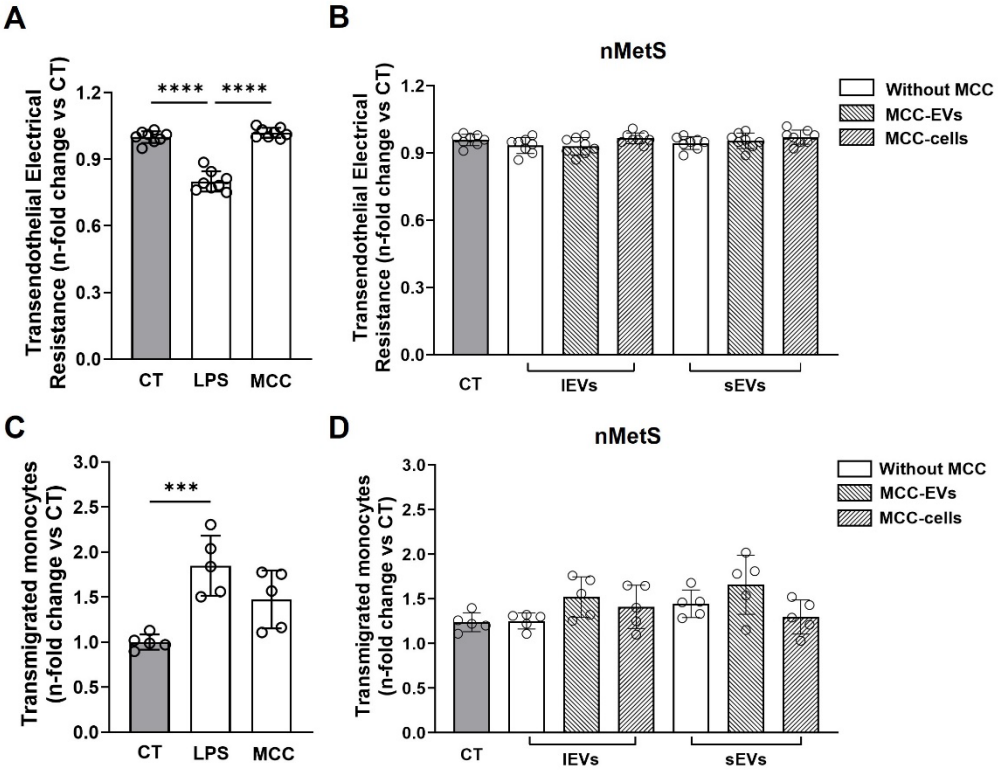

Supplementary Figure 3. Effect of LPS, MCC950 and non-metabolic syndrome (nMetS)-extracellular vesicles (EVs) on endothelial permeability and monocyte transmigration. A and B, Changes on endothelial permeability measured by transendothelial electrical resistance induced by (A) lipopolysaccharide (LPS, 5µg/mL) and MCC950 inhibitor (MCC, 1 µg/mL), (B) large EVs (lEVs) or small EVs (sEVs) from nMetS subjects in the absence of MCC, after MCC preincubation of EVs (MCC-EVs) or previous MCC treatment of cells (MCC-cells) (n=8). C and D, Transmigration of monocytes through an endothelial cell monolayer induced by (C) LPS and MCC, (D) lEVs or sEVs from nMetS subjects. EVs (MCC-EVs) or cells (MCC-cells) were pre-incubated with MCC950 (1 µg/mL) (n=5). Data are expressed as mean ± SD. Statistical significance was tested with 1-way ANOVA and Tukey post hoc test between all conditions for each panel. ***p<0.001 and ****p<0.0001.

Supplemental Figure 4
(Vidal-Gomez et al.)

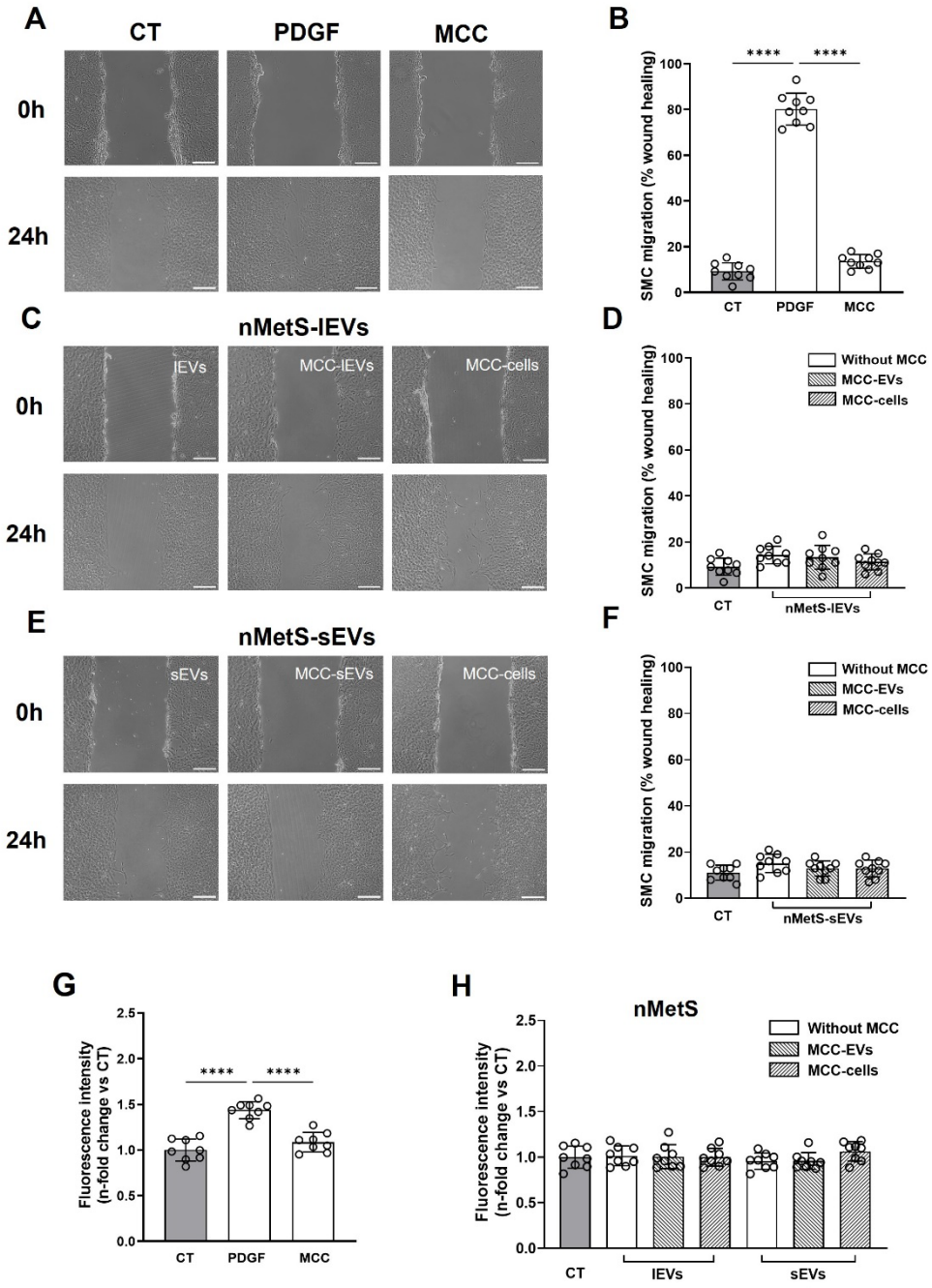

Supplementary Figure 4. Effects of PDGF, MCC950 and non-metabolic syndrome (nMetS)-extracellular vesicles (EVs) on smooth muscle cell (SMC) migration and proliferation. A-F, Representative microscopic images and quantification of SMC migration in response to (A-B) PDGF (25 µg/mL) or MCC950 (MCC, 1 µg/mL), (C-D) large EVs (lEVs) or (E-F) small EVs (sEVs) from nMetS subjects. EVs (MCC-EVs) or

cells (MCC-cells) were pre-incubated with MCC (1 µg/mL) (n=9, scale-bar size: 200 µm). G and H, Effects of PDGF (G), MCC, (H) lEVs or sEVs from nMetS subjects on the number of SMC measured by CyQuant Kit. EVs (MCC-EVs) or cells (MCC-cells) were pre-incubated with MCC (1 µg/mL). Histograms show the fold-change to the control (CT) on fluorescence intensity representing the changes in cell number (n=8). Data are expressed as mean ± SD. Statistical significance was tested with 1-way ANOVA and Tukey post hoc test between all conditions for each panel. ****p<0.0001.

Supplemental Figure 5
(Vidal-Gomez et al.)

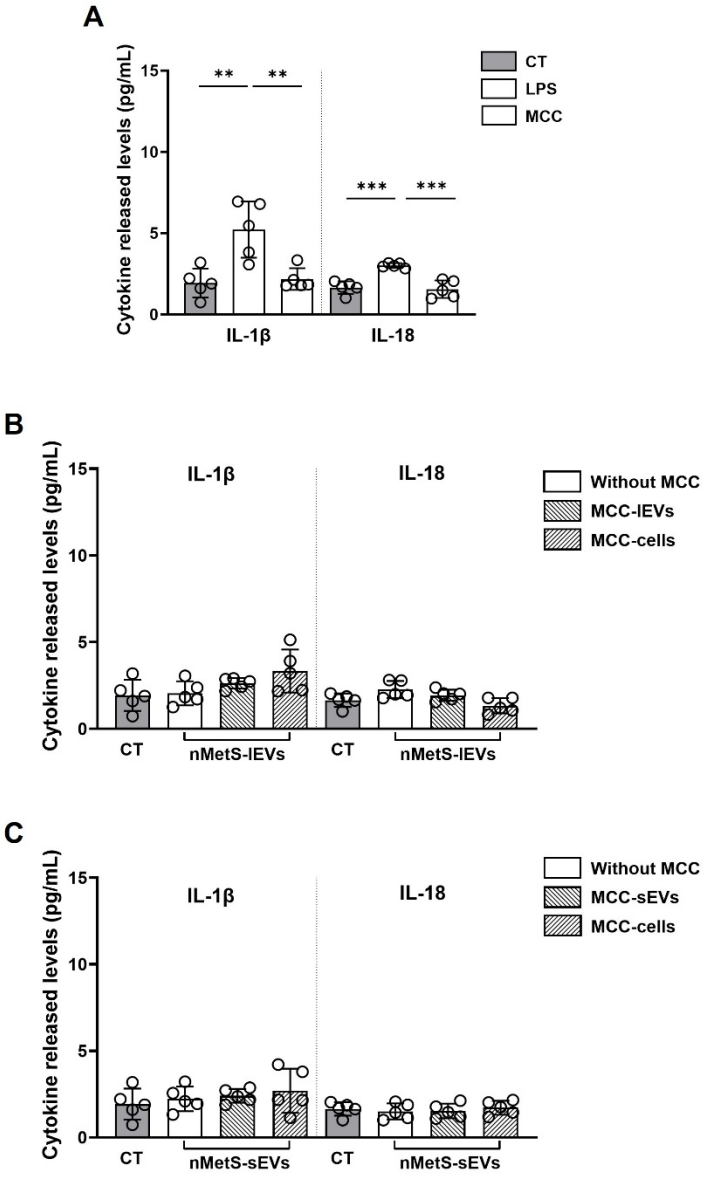

Supplementary Figure 5. Effects of lipopolysaccharide (LPS), MCC950 and non-metabolic syndrome (nMetS)-extracellular vesicles (EVs) on smooth muscle cell (SMC) secretion of interleukin (IL)-1β and IL-18. Secretion of IL-1β and IL-18 by SMC in response to (A) LPS (5μg/mL) and (MCC, 1 μg/mL), (B) large EVs (lEVs) or (C) small EVs (sEVs) from nMetS subjects in the absence or after MCC preincubation of EVs (MCC-EVs) or previous MCC treatment of cells (MCC-cells). Histograms show the normalized fold-change to the control (CT) on cytokine release representing the

changes in IL-1β and IL-18 levels (n=5). Data are presented as mean ± SD. Statistical significance was tested with 1-way ANOVA and Tukey post hoc test between all conditions for each panel. **p<0.01 and ***p<0.001.

Supplemental Figure 6
(Vidal-Gomez et al.)

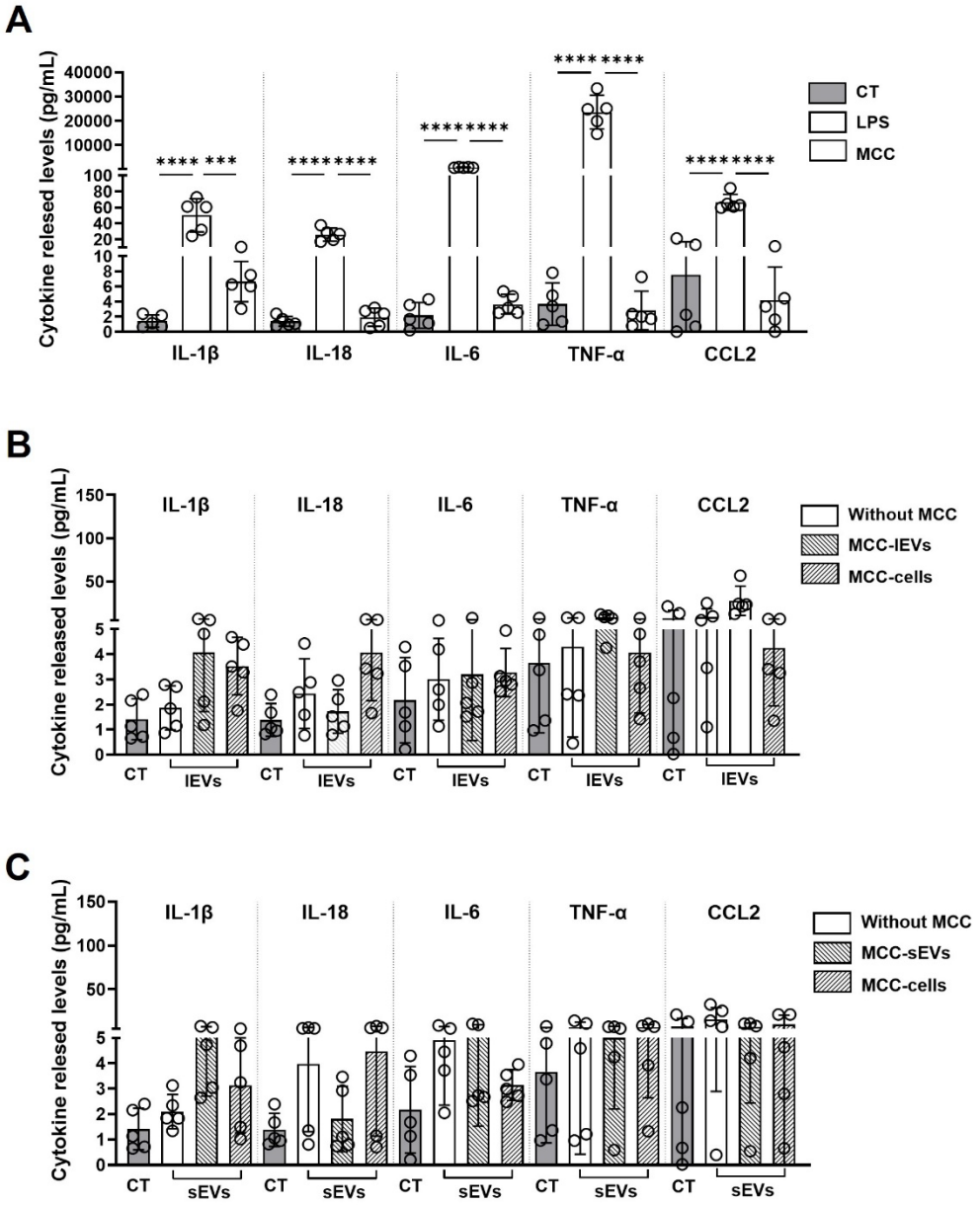

Supplementary Figure 6. Effect of lipopolysaccharide (LPS), MCC950 and non-metabolic syndrome (nMetS)-extracellular vesicles (EVs) on macrophage proinflammatory cytokine secretion. Cytokine secretion by human monocyte-derived macrophages in response to (A) LPS (1 μg/mL) and MCC950 (MCC, 1 μg/mL), (B) large EVs (lEVs) or (C) small EVs (sEVs) from nMetS subjects in the absence or after MCC preincubation of EVs (MCC-EVs) or previous MCC treatment of cells (MCC-cells). Histograms show the fold-change to the control (CT) of cytokine release

representing the changes in interleukin (IL)-1β, IL-18, IL-6, tumor necrosis factor (TNF)-α, and chemokine (C-C motif) ligand 2 (CCL2) levels (n=5). Data are expressed as mean ± SD. Statistical significance was tested with 1-way ANOVA and Tukey post hoc test between all conditions for each panel. ****p<0.001.

Supplemental Figure 7
(Vidal-Gomez et al.)

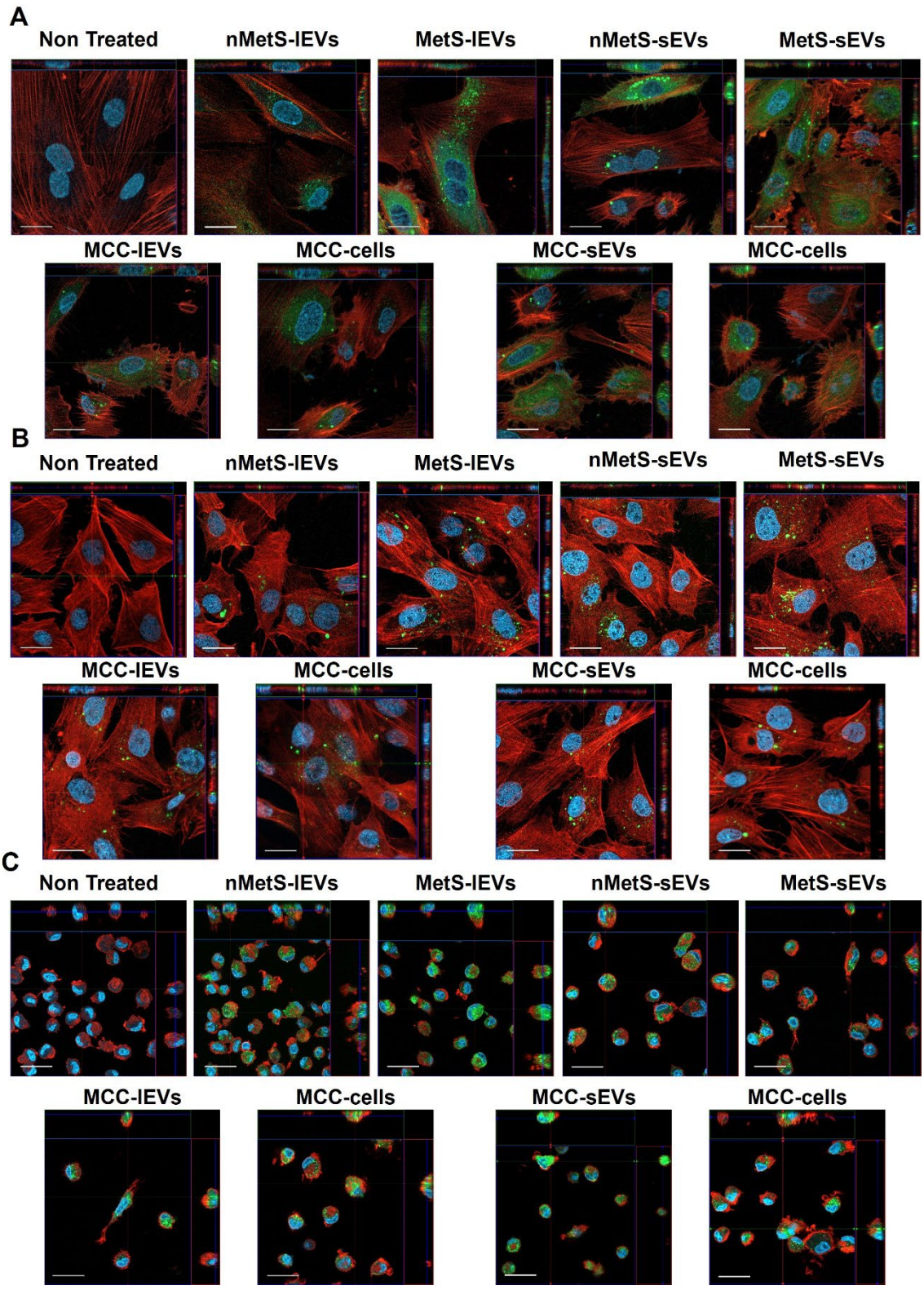

Supplementary Figure 7. Internalization of large (lEVs) or small extracellular vesicles (sEVs) from non-metabolic syndrome (nMetS) and metabolic syndrome

(MetS) patients by cells. Representative confocal images of PKH67-labeled EVs from nMetS and MetS (in green) internalized into human aortic endothelial cells (A), human aortic smooth muscle cells (B) and human monocyte-derived macrophages (C), in the absence of the NLRP3 inhibitor MCC950 (MCC, 1 µmol/L) or after the pre-incubation of EVs (MCC-lEV and MCC-sEVs) or cells (MCC-cells). Cells were labelled with Phalloidin-A568 (in red), nucleus of cells with Dapi (in blue) (n=3). Horizontal scale bar =20 µm.

Supplemental Figure 8
(Vidal-Gomez et al.)

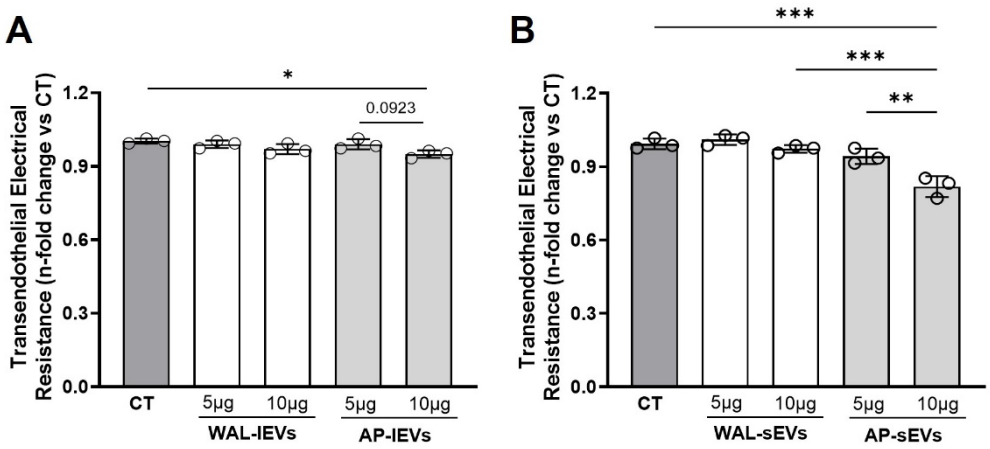

Supplementary Figure 8. Effects of extracellular vesicles (EVs) from human atherosclerotic plaque (AP) on endothelial permeability. Changes on endothelial permeability measured by transendothelial electrical resistance induced by lEVs (A) and sEVs (B) from wall adjacent to the lesion (WAL) and AP (5 and 10 µg/mL) (n=3). Statistical significance was tested with 1-way ANOVA and Tukey post hoc test between all conditions for each panel. *p<0.05, **p<0.01 and ***p<0.001.